1. The LSST White Dwarf Model Sample

In order to generate a simulated sample of disk and halo white dwarfs, four sets of quantities need to be adopted:

1. The spatial distribution
2. The distributions of three velocity components
3. The bolometric luminosity function
4. The mapping from bolometric luminosity to broad-band luminosity in each LSST bandpass

We proceed with detailed descriptions of the adopted quantities.

1.1. The Spatial Distribution

LSST will detect white dwarfs over a distance range much larger than the disk scale heights and lengths. Hence, the spatial variation of volume density must be taken into account. We assume that the spatial distribution of white dwarfs traces the distribution of main-sequence stars, both for halo and disk populations. The spatial distribution of main-sequence stars was recently mapped in detail using SDSS data by Jurić et al. (2008, hereafter J08). J08 also provided the best-fit parameters for a Galaxy model based on two exponential disks and a power-law halo. They showed that the stellar number density distribution, $\rho(R, Z, \phi)$ can be well described (apart from local overdensities; the J08 best-fit was refined using residual minimization algorithms) as a sum of two cylindrically symmetric components

$$\rho(R, Z, \phi) = \rho_D(R, Z) + \rho_H(R, Z). \quad (1)$$

The disk component can be modeled as a sum of two exponential disks

$$\rho_D(R, Z) = \rho_D(R_\odot, 0) \left[\mathrm{e}^{-|Z+Z_\odot|/H_1 - (R-R_\odot)/L_1} + \epsilon_D \mathrm{e}^{-|Z+Z_\odot|/H_2 - (R-R_\odot)/L_2} \right], \quad (2)$$

and the halo component requires an oblate power-law model

$$\rho_H(R, Z) = \rho_D(R_\odot, 0)\, \epsilon_H \left(\frac{R_\odot^2}{R^2 + (Z/q_H)^2} \right)^{n_H/2}. \quad (3)$$

The best-fit parameters are discussed in detail by J08. We have adopted the following values for parameters relevant in this work (second column in Table 10 from J08): $Z_\odot$=25

pc, $H_1 = 245$ pc, $H_2 = 743$ pc, $\epsilon_D = 0.13$, $\epsilon_H = 0.0051$, $q_H = 0.64$, and $n_H = 2.77$. The normalization $\rho_D(R_\odot, 0)$ for white dwarfs is implicit in the adopted luminosity function (see below).

1.2. The Kinematic Distributions

We assume that the kinematics (distributions of three velocity components) of white dwarfs is the same as the corresponding distribution of main-sequence stars, both for halo and disk populations. Ivezić et al. (2008, hereafter I08) and Bond et al. (in prep.) extended the J08 analysis to kinematic space. They showed that the overall gross behavior of stellar kinematics can be well described (apart from local overdensities) as a sum of two components, disk and halo, that map well to components detected in spatial profiles and metallicity distribution. The non-rotating halo component has by and large spatially uniform Gaussian kinematics, with dispersions of $\sigma_R = 135$ km/s, $\sigma_\phi = 85$ km/s, and $\sigma_Z = 85$ km/s (with uncertainties of about 10 km/s). The disk kinematics are dominated by a vertical (Z) gradient. The velocity dispersions in the R and Z directions can be modeled as relatively simple functions of the form $\sigma = a + b|Z|^c$ (see Table 1). The best-fit *median* rotational velocity for disk stars in the $|Z| = 0.8 - 5.0$ kpc range and $R \sim 8$ kpc, is

$$v_{median}^{disk}(Z) = -205 + 19.2\,|Z/\mathrm{kpc}|^{1.25}\ \mathrm{km/s}. \tag{4}$$

We assume that this relation is valid all the way to $Z = 0$. Unlike the other two components (R and Z), the *shape* of the rotational velocity (v_ϕ) distribution for disk stars is non-Gaussian. It can be modeled, in the $|Z| = 0.8 - 5.0$ kpc range and for $R \sim 8$ kpc, as a sum of two gaussians,

$$p_D(x = v_\Phi|Z) = 0.25\,G[x|\mu_1(Z), \sigma_1(Z)] + 0.75\,G[x|\mu_2(Z), \sigma_2(Z)], \tag{5}$$

where the means are

$$\mu_1(Z) = v_{median}^{disk}(Z) - 23\ \mathrm{km/s}, \tag{6}$$

and

$$\mu_1(Z) = v_{median}^{disk}(Z) + 11\ \mathrm{km/s}. \tag{7}$$

Similarly to the R and Z velocity dispersions, the widths can be described by $\sigma = a + b|Z|^c$, with the best-fit coefficients listed in Table 1.

We adopt these results for generating the three velocity components of halo and disk white dwarfs.

1.3. The White Dwarf Luminosity Function

For disk stars, we adopt the measured luminosity function based on SDSS data (Harris et al. 2006). Using their Figure 4, we obtained the following parameters for a power-law appoximation to the measured Φ (the number of white dwarfs per cubic parsec and magnitude)

$$\begin{aligned} \log(\Phi) &= -2.65 + 0.26\,(M_{\rm bol} - 15.3) \quad \text{for } 7 < M_{\rm bol} < 15.3 \\ \log(\Phi) &= -2.65 - 1.70\,(M_{\rm bol} - 15.3) \quad \text{for } 15.3 < M_{\rm bol} < 17.0, \end{aligned} \tag{8}$$

with n which agrees with the data to within 10% at the faint end. The observational knowledge of halo white dwarf luminosity function is much poorer. Theoretical predictions indicate an overall shift of the halo luminosity distribution towards fainter absolute magnitudes. Motivated by these predictions, we simply shift the Harris et al. luminosity function by 0.7 mag.

1.4. The White Dwarf Spectral Energy Distribution

We use models by Bergeron et al. (2005), which are in good agreement with SDSS measurement (Eisenstein et al. 2006). Using a sample of white dwarfs with SDSS spectra, Eisenstein et al. found a very narrow distribution (0.1 dex) of log(g) centered on log(g)=7.9. Motivated by this result, we adopt log(g)=8.0 for all white dwarfs in the simulated sample.

Table 1. Best-fit parameters for the R and Z velocity dispersion for disk stars, $\sigma = a + b|Z|^c$.

direction	a	b	c
R	40	5.0	1.5
Z	25	4.0	1.5
ϕ_1	12	1.9	2.0
ϕ_2	34	0.7	2.4

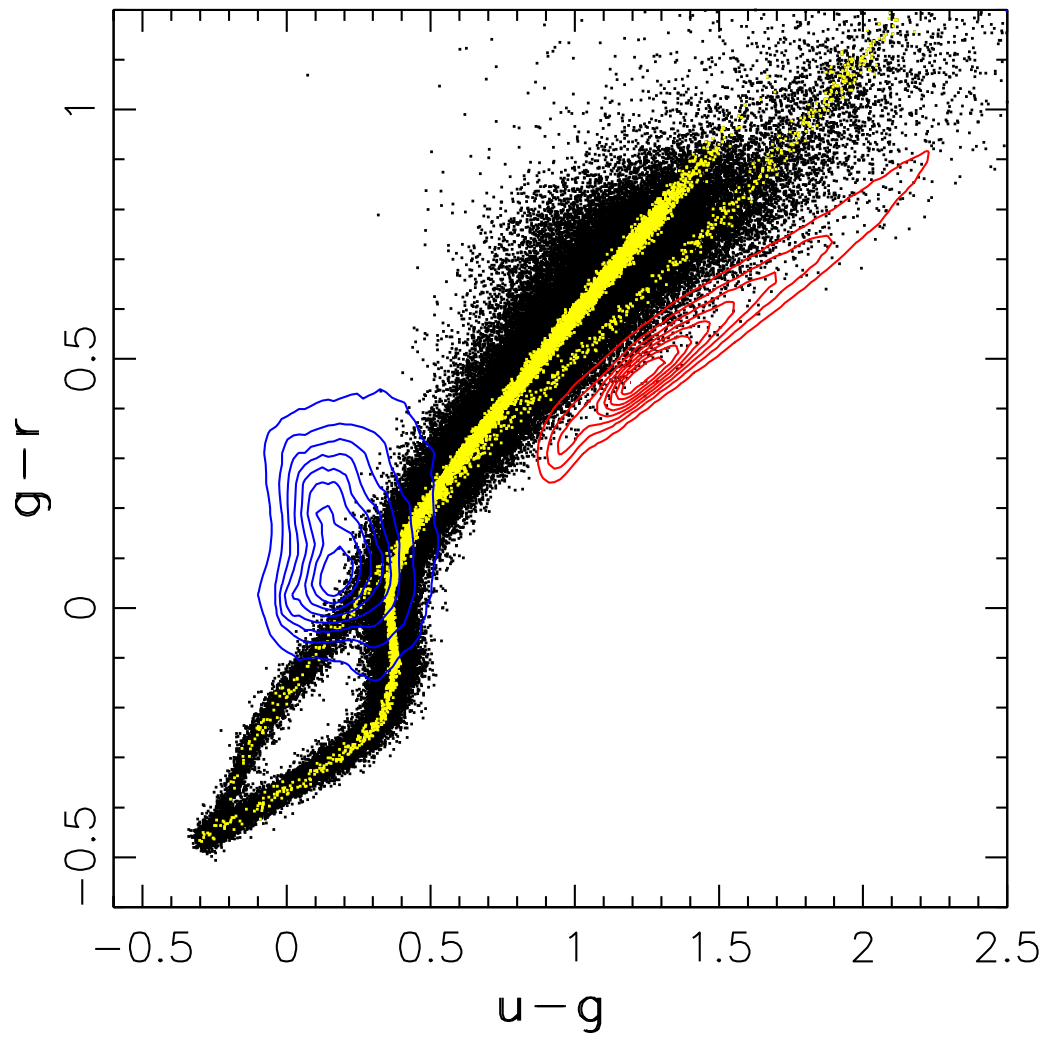

Fig. 1.— The distribution of the simulated white dwarfs in the $g - r$ vs. $u - g$ color-color diagram. Black points show objects with $r < 24.5$ and $b > 60°$. Yellow points show a subsample of, predominantly brighter, sources that have 10σ or better "measurement" of the trigonometric parallax. The two sequences correspond to He and H white dwarfs. The distribution of low-redshift ($z < 2.2$) quasars observed by SDSS is shown by blue contours. The blue part of the stellar locus (dominated by F and G stars), as observed by SDSS, is shown by the red contours.

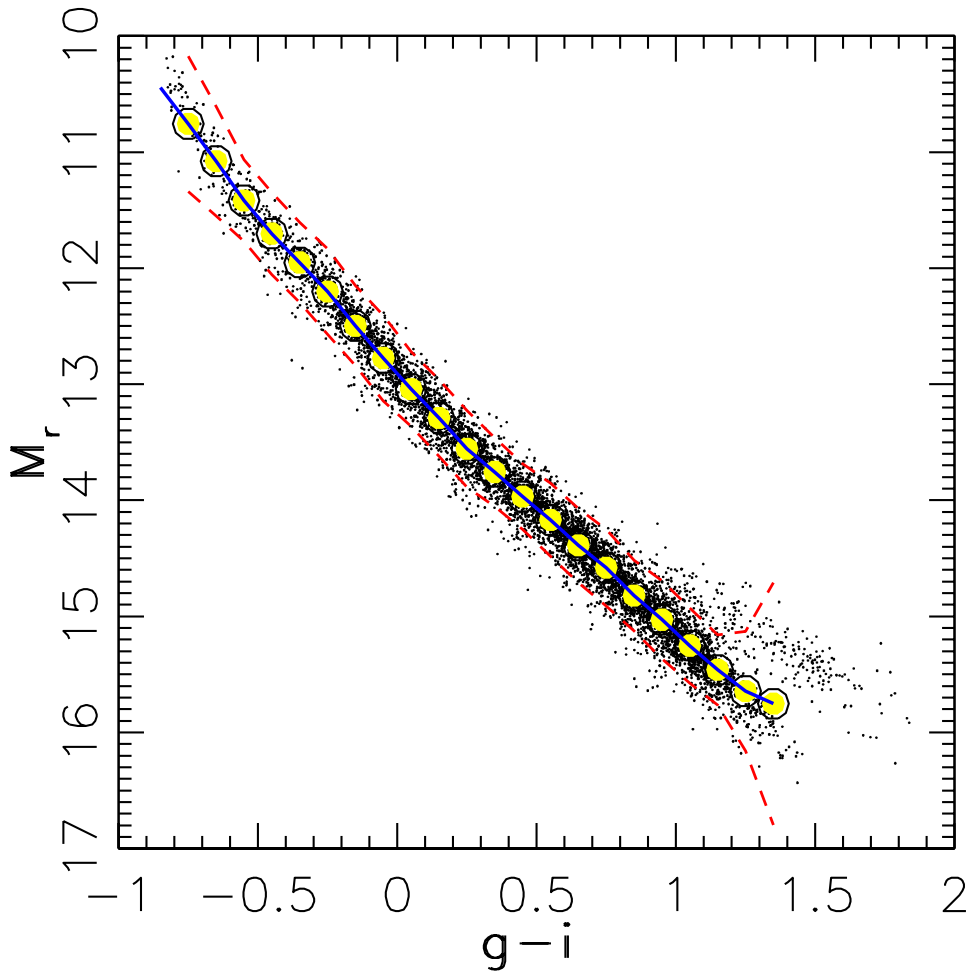

Fig. 2.— The calibration of photometric parallax relation, $M_r(g-i)$, for white dwarfs. Black points show objects that have 10σ or better "measurement" of the trigonometric parallax (same objects as shown by yellow points in Figure 1). The "bifurcation" seen at the red end is due to differences between H and He dwarfs. The large yellow points show the median M_r values in 0.1 magnitude wide $g-i$ bins, and the red lines show the $\pm 2\sigma$ envelope around the medians. The blue line shows the $M_r(g-i)$ relation used to generate the simulated sample.

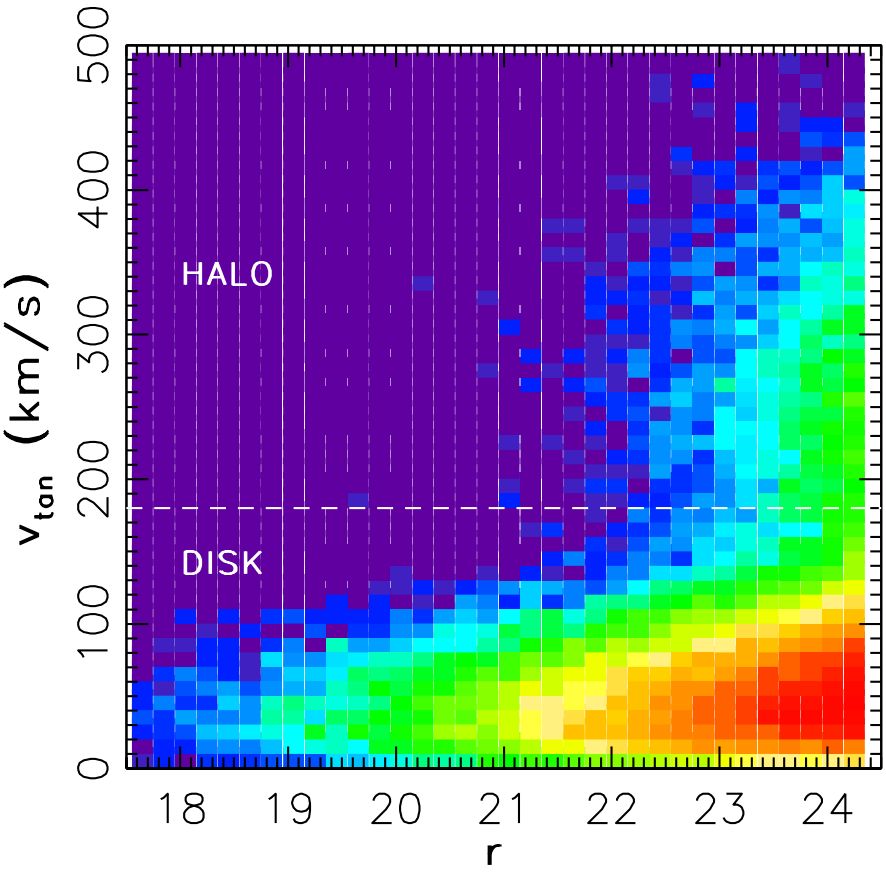

Fig. 3.— The dependence of tangential velocity on apparent magnitude for white dwarfs with $b > 60°$. The map shows counts of stars in each bin shown on logarithmic scale (increasing from blue to red). The tangential velocity is computed from proper motion and distance determined using photometric parallax relation shown in Figure 2. At faint magnitudes ($r > 20$) the sample contains a large fraction of halo dwarfs. The horizontal line at 180 km/s is adopted cutoff for isolating a clean sample of halo stars (contamination by disk stars is below 10%).